Grumman Research Department Report RE-306

RESEARCH ON GAS-SURFACE INTERACTIONS 1966-67

PART II - NUMERICAL EXPERIMENTS ON SCATTERING OF NOBLE GASES FROM SINGLE CRYSTAL SILVER

by

R. A. Oman

Fluid Mechanics Section

November 1967

Final Report on Contract NASw-1461
Fluid Dynamics Branch
Office of Advanced Research and Technology
NASA, Washington, D. C.

Prepared by Research Department
Grumman Aircraft Engineering Department
Bethpage, N. Y. 11714

Approved by: Charles E. Mack, Jr.
Charles E. Mack, Jr.
Director of Research

ABSTRACT

Three dimensional numerical experiments on the scattering of noble gas atoms from single crystal surfaces of silver are described. This numerical method can be very useful in determining the relative importance of different variables in the interactions, although it cannot be expected to give quantitative agreement with individual cases until a better knowledge of the interatomic binding energies and the surface state is available. Most of the cases are for neon on the fcc (111) surface, but isolated cases of helium and argon on (111) and neon on (100) are included. The energies include those of effusive molecular beams from 300°K to 45,000°K equivalent source temperatures (.06 to 7.8 eV). Several interaction parameters describing mean energy and momentum exchanges and traces of the spatially resolved flux in the incident plane are given for most of the cases. Sample out-of-plane flux data and some typical data on spatially resolved energy are also given, and general trends for the rest of the data are described. The results give trapping probabilities that are much greater than those inferred from laboratory experience, and flux patterns that are significantly broader than those encountered in the experiments for the few cases that can be compared directly. The neon trends with increasing energy are quite similar to those of the Saltsburg and Smith experiments for xenon, with new effects

appearing in the present results for energies higher than those of the laboratory experiments. These new effects include multiple peaks, one above and one below specular, and a broadening of the patterns with increasing incident energy. They are attributed to increased resolution of the surface atomic configuration due to deeper penetration of the potential field above the surface. The trends of the Logan, Keck and Stickney hard cube theory are shown in the present results at low incident energy, and the expected hard sphere limit behavior is observed at very high incident energy, in agreement with the recent calculations of Goodman.

TABLE OF CONTENTS

LIST OF ILLUSTRATIONS

INTRODUCTION

Recent developments in molecular beam and related experimental techniques have made possible the measurement of spatial distributions of flux in gases reflected from well characterized solid surfaces.[1-3] In particular Saltsburg and Smith have developed an important technique for constructing epitaxial crystal surfaces as the molecular beam experiment is carried out, and have been able to achieve a moderate range of energies in their incident beam. At the same time, several techniques for numerical computation of gas surface interactions at high incident energies have been developed by the author and his colleagues,[4] by Goodman [5] and Erofeev,[6] and more recently by Raff, Lorenzen, and McCoy.[7] These methods have become quite complex, and reflect most of the known features of the ideal surface state; but their results can be no better than the poor quality of our knowledge of interatomic forces and real surface configurations. The greatest value in numerical experiments lies in the ability to vary parameters independently and thereby isolate the controlling mechanisms in each interaction regime. They also provide the ability to measure any desired property at any point in the process without changing the interaction, a feature that no laboratory experiment offers. They fail to give in their numerical output the insight that is contained in even the crudest analytical theory, so they must be supplemented

by simpler theoretical models if their product is to be useful for many different cases. They are also limited by the lack of reality in the basic computer model, so they must be continually reworked after testing against suitable laboratory experiments. Computation time is always a limiting factor, but recent improvements in computing machinery have made possible very detailed studies. We now get 6 trajectories per minute on an IBM 360-75.

Although all the published numerical methods can give results for mean momentum and energy exchanges, only Goodman's method has heretofore been able to resolve three dimensional trajectories into spatial distributions. However, since his calculations deal with a modified hard sphere model which portrays the limit of very high energy, they have only limited usefulness for comparison with low and moderate energy data from molecular beam scattering. By a new interpolation technique, we have recently been able to produce spatial distributions of density, mass flux, and energy flux which qualitatively represent in three dimensions the results of trajectory computations with as few as 50 trajectories in a sample. This technique has been applied to computation of the interaction of He, Ne, and Ar with Ag single crystal surfaces. The present model includes a modeling of thermal motion in the crystal, a first approximation to the effects of restraining forces in the lattice, an attempt to portray the interatomic potentials in a realistic form (a Lennard-Jones 6-12), and the correct lattice structure for

an ideal fcc crystal. We expect moderately good results for the computation down to an incident energy of a few tenths of an eV where, for most combinations of gas and solid species, the probability of trapping gets very high, the long collision times create serious errors due to the assumption of independent oscillators, and the errors in determining interatomic potentials become very important.

The classical theory of Logan, Keck, and Stickney[8] — often called the hard cube theory — has enjoyed notable success in explaining the trends of existing scattering data, both in the spread of the scattered lobe and in the direction of the maximum. There are two basic reasons for this, both having to do with the limited energy range of the present generation of "clean-surface" data. In all existing experimental cases, the mean thermal energy of a lattice atom has been of the same order as the energy of the incident molecules, so that the vertical oscillations of the lattice, which are central to the hard cube theory, are also the most important effect in the scattering. In addition, since there is insufficient translational energy in the incident molecule to allow it to penetrate deeply into the repulsive portion of the interatomic potentials, the equipotential surface seen by the incident particle at its greatest penetration of the potential field should be quite smooth. These features apparently combine to produce a scattering pattern that is quite sharp and near the specular

direction. As the ratio of gas energy to lattice thermal energy increases from a low value, the lobes become sharper and lie closer to the surface. Two important points must not, however, be overlooked. Neither the experiments nor the original hard cube theory can determine the fraction of particles that is trapped on the surface for more than a few lattice vibration periods; and the hard cube theory must use empirical adjustments if it is to describe the effects of scattering from the crystal atomic structure, effects which should become quite important at higher incident energy, E_i. Evidence from a large number of cases computed by the author and co-workers[4] indicates that trapping should have been the predominant result in all the data of Saltsburg and Smith for Ar and the heavier gases; these trends are corroborated by the calculations of Jackson[9] and Madix and Korus,[10] each of whom used radically different approaches. Madix and Korus have introduced a trapping mode into the hard cube theory, and find trapping probabilities comparable to present results for comparable values of ϵ. In addition, the trajectory calculations of Goodman[5] and Jackson[9] agree with our general observation that at high E_i the scattered distributions are quite broadly dispersed. Erofeev's theory[6] gives results that are even more diffuse, although they retain some memory of the incident direction. Since the trend of lobe shape and direction with increasing E_i in the experiments is in the opposite direction, doubt has been cast on the validity

of many assumptions inherent in our trajectory computations and those of the other authors cited.

This paper will show that consideration of all the mechanisms known to be important produces a set of scattering patterns that exhibits many of the trends of the earlier experiments, except that the laboratory experiments do not appear to show the theoretically predicted high trapping probabilities, and give somewhat sharper peaks at low E_i. At the same time the calculations reproduce the highly scattered cases expected for high E_i in a completely straightforward manner. Comparison with phenomenological models enables us to visualize some of the dominant mechanisms in each case so that some of the reasons for the observed behavior can be understood. A particularly interesting feature of the present results is the frequent occurrence of multiple lobes — a feature also noted by Jackson.[9] None of our attempts to explain this separation of lobes has been successful.

TRAPPING AND ADSORPTION

It is important to delineate the role of the trapped particle in the computations and in the experiments, particularly since trapping is such a common result in the theory. Although the following points have been discussed in our previous papers[4] and by several others (notably Goodman[11]), there are special features to be emphasized here.

We use the term "trapping" to denote the process by which a particle loses its ability to escape from the lattice without first acquiring additional energy from the thermal motion of the lattice. Thermal motion may also have a substantial effect on untrapped particles, the distinguishing feature being the temporary state of negative total energy for those that are trapped. The subsequent reemission of the trapped particle then becomes a problem in desorption mechanics. We traditionally assume, somewhat arbitrarily, that the ultimate state of reemission of a trapped particle will be Maxwellian at the surface temperature, and that the net energy exchanged with the lattice must account for the energy of reemission of the trapped fraction. We have included this contribution (a loss by the wall of $2kT_w$ per atom) in the results for energy transmitted to the lattice, E_ℓ. It is important to note this, since many applications of interest do not allow reemission, and appropriate corrections must be made. In all the momentum coefficients we quote, the trapped fractions have been excluded, so that we are dealing only with those particles that are not trapped (although they may have hit many lattice atoms in their encounters with the wall).

As to the mechanism of trapping, we can easily visualize an acceleration by the attractive field of the lattice, followed by a primary scattering collision. If the energy equivalent of the normal momentum after the collision (i.e., $p_z^2/2m$) is not

sufficient to overcome the attractive effect of the lattice, the particle will be condemned to a second scattering collision. Except for those cases in which $kT_w \gg \epsilon$, most such particles will be eventually trapped. The binding energy ratio, ϵ/E_i, the angle of incidence, θ_i, the mass ratio, μ, and the wall temperature ratio, kT_w/E_i, all play major roles in this process.

The role of trapping in the molecular beam experiments of Saltsburg and Smith[1] poses an especially difficult and important question. Their phase-sensitive detector does not detect particles with long residence times on the surface, and they have not been able to integrate their exit flux over the entire exit hemisphere. Since it would be unreasonable to expect any large fraction of the trapped particles to retain memory of their incident state, and since lobes in the specular region are always present on freshly deposited surfaces, Saltsburg and Smith infer from the qualitative nature and the levels of their signals that trapping is not the dominant result in any of their experiments. This question is relevant to the comparisons with all theories that include trapping, and merits further study.

SCATTERING CALCULATIONS

The numerical computations of gas-surface interaction discussed here were conducted in three parts. The first was the computation of the atomic trajectories themselves, carried out by

numerical integration of the classical equations of motion in three dimensions for a family of point-mass sources of potential, which are directed toward a model crystal surface. Some of the cases were done on an IBM 7094, some on an IBM 360-75. Figure 1 shows the coordinate system. The aiming points of the individual trajectories are uniformly distributed over a unit cell surface. Although several optional models are available within the same computer program, all the results in this paper were produced by using fcc (111) and a few (100) configurations of lattice atoms, monatomic gas molecules, active thermal motion in the lattice, random distributions of incident azimuth angle φ_i (i.e., between trajectory computations the crystal was rotated relative to the incident beam about the surface normal through an arbitrary angle). The computations are based on the assumption that each of the 50 or 98 lattice atoms considered oscillates independently of its neighbors. The isotropic lattice forces are assumed to be those of linear springs, and the natural frequency is estimated as the highest characteristic frequency in the Debye spectrum of the solid. The model for thermal motion imposes identical energies in each independent direction (i.e., x, y, z) for each lattice oscillator. Each phase angle is randomly selected, which gives us a complete equipartition and random motion but a thermodynamically naive model. Additional computational details may be found elsewhere.[4] The output is in the form of a scattered sample of gas

atoms, some of which may become trapped, with their exit velocities described by their speed and their exit angles measured as in Fig. 1. In this paper we will refer to φ as measured from the plane of incidence when discussing the results, in reality dealing with $\varphi_{exit} - \varphi_i$.

The second part of the over-all computation employs the results of the scattering calculation to generate a spatial distribution of reflected atoms from the finite number of trajectories calculated for a given case. First, the fraction of trapped particles is recorded and these particles are discarded from the sample. Second, each trajectory is matched by an artificially generated twin located at those exit coordinates that are symmetric with respect to the plane of incidence. Third, each trajectory is replaced by a distribution function $f(\theta, \varphi)$ that expresses the probability of finding that particle at a particular exit coordinate (θ, φ). Each molecular trajectory in the exit distribution thus represents the final state of an infinite population of incident particles uniformly distributed over a non-repetitive subunit of the surface. Since a complete set of these subunits comprises a repetitive unit of the surface, we generate one trajectory for each of the N aiming points on a uniform grid spaced over the smallest repeating dimension of the lattice structure. The aiming point grid is so fixed relative to the crystal that it does not shift with changes in azimuth angle. If we aim

at the grid point with initial conditions specified at infinity, we do not, in general, contact the lattice at the aiming point, but find instead that randomness is introduced by the long-range forces from the semi-infinite crystal (these forces are included in the trajectory computations), by thermal motion of the lattice, by the randomly selected φ_i, and by the (unknown) change in scattered angle resulting from change in aiming point and approach angle. From experience,[4,5] we find that this procedure yields mean interaction parameters that are not too sensitive to small changes in aiming point (i.e., the incident particles have large effective diameters).

Lacking a complete knowledge of the distribution function for each subunit, we assume that the properties of the resulting trajectories are the mean properties for the corresponding subunit trajectories, and that the subunit trajectories are normally distributed; viz.,

$$f(\theta, \varphi) = Av_j^{-1} \exp(-Bz_j^2) , \qquad (1)$$

where z_j is the great-circle arc between (θ_j, φ_j) and (θ, φ) on the unit hemisphere centered at the origin, and v_j is the ratio of the exit velocity of the j^{th} particle to the incident velocity of all of the particles. The relationship between parameters A and B is determined by requiring the fraction of the incident flux that exits in a unit solid angle to have a mean value

of unity when averaged over the entire exit hemisphere. For a sample of N particles with a sufficiently good resolution (i.e., large N), this calculation becomes

$$2\pi = 2\pi N \int_c \sin c f_j(c) v_j \, dc \approx 2\pi N \int_0^\infty A \sin c \, e^{-Bc^2} \, dc \qquad (2)$$

where c represents the great-circle arc from the direction (θ_j, φ_j) to (θ, φ).

The form of Eq. (2) normalizes f so that it expresses the density distribution function per unit solid angle. The flux distribution per unit solid angle $q(\theta, \varphi)$ is then given by

$$q(\theta, \varphi) = A \sum_{j=1}^{N} e^{-Bz_j^2}$$

where

$$z_j = \cos^{-1}[\cos\theta \cos\theta_j + \sin\theta \sin\theta_j \cos(\varphi - \varphi_j)]$$

$$A \approx \frac{2}{N}\left[\frac{1}{B} - \frac{1}{3!B^2} + \frac{2}{5!B^3} \cdots\right],$$

and

$$B = N/2\pi\xi \, .$$

The parameter ξ is an arbitrarily chosen resolution constant. As ξ increases, the resulting distribution becomes smoother and resolution decreases. Freedom in the choice of ξ is analogous to freedom of choice in the size of cells if we were to construct a distribution function by counting trajectories in each of a large number of cells on the exit sphere, a procedure for which the existing number of trajectories is hopelessly inadequate. The value of ξ used here ($\xi = 2.0$) has been chosen so that a uniform spacing of N particles over 2π steradians produces a fluctuation in q over the exit hemisphere of no more than a few percent. Somewhat higher resolutions could be employed, but they would give rise to false fluctuations in sparsely populated regions.

The test of the method is its ability to reproduce the general character of the distribution as additional cases with the same input variables are added. Reproducibility varies with many factors, of which by far the most important is the number of trajectories in the sample. Many combinations of statistical samples have been tried, with results ranging from poor to excellent. The qualitative nature of the distributions is reproducible for samples of 50 or more trajectories in most cases tested, but quantitative reproducibility cannot be expected until sample sizes are well in excess of 100. Some of the poorer cases tested are shown in Fig. 2, which also shows independent (i.e., different sets of random variables) sets of 50 trajectories and their combination.

There is a general tendency for reproducibility to improve with increasing E_i. This is due partly to greater yield (i.e., trapping no longer reduces the number of usable particles), and partly to increased directivity. The distributions are never as widely dispersed as when they are thermally scattered at very low E_i. Increased dispersion leads to a less reliable local value for each of the moments.

All the results shown in Figs. 3 through 15 were derived from samples of 50 or more, except for Ne at 22,400 and 44,800°K, which were derived from 32. Note that the present spatial distribution data cannot be expected to give quantitatively reliable results. The trends with changes in conditions, the general character of the distributions, and the mean values of interaction parameters for given incident states are the only kinds of information that we can expect to have quantitative reliability, and then only at higher energy levels.

In the third step of the over-all investigation we applied the results of phenomenological analysis to the same input conditions and compared fractions trapped and energy exchanged. These procedures have been described in our previous papers.[4] The results are shown in Figs. 3 and 4. Note that as yet there is no correlating model for momentum distributions shown in Figs. 5 through 7, although Goodman[5] presents some correlations for momenta in the hard sphere limit.

SELECTION OF TEST CONDITIONS

We chose to perform some of our calculations under the experimental conditions employed by Saltsburg and Smith.[1] Although the data of Hinchen and Shepherd[2] are excellent, they offer only conditions of 300°K incident gas temperature, and as we show below, the high trapping probability encountered in the calculations for low E_i makes it difficult to treat these cases directly with our method. Other published data use polycrystalline and/or dirty surfaces. Of the data published by Saltsburg and Smith, the most trustworthy surfaces appear to be the epitaxially grown Ag (111) surfaces used with the noble gases. Because the interatomic potential parameters are not known and the incident beam contained a distribution of energies with a most-probable value of $2kT_i$ instead of a monoenergetic beam, we should not expect more than qualitative agreement between the experimental scattering patterns and the results from our computer experiments, even if the model were perfect. At the low energies used here, we may also encounter serious errors due to the inaccuracy of the independent-oscillator lattice model employed for these calculations ($\omega_n \tau_c$ is often much greater than unity), as well as to the importance of the lattice thermal motion, which is only crudely portrayed in the present model. The low energy helium case is probably also in error because of quantum effects. We have employed a constant $E_i = 2kT_i$ for each case and have fixed the surface temperature at the value

used to ensure epitaxial growth (560°K) in the experiments. The lattice structure used in most cases was fcc (111), and two values for the Debye temperature were selected to determine the strengths of lattice restoring forces. In some cases we employed the accepted bulk value for Ag of 225°K, while in others we followed the rule for surface corrections to Debye temperatures advanced by Lyon and Somorjai,[12] namely, that the surface region has a Debye temperature value very near one-half that of the bulk. This alteration may have a substantial effect in some dynamic ranges since the exponent that portrays the effect of restoring forces in the model equations[4] will decrease by a factor of 4, which leads to a larger predicted energy exchange in the primary collision with the surface, and a corresponding decrease in the expected normal momentum recovery at the surface. It also affects thermal velocities of the surface atoms.

There are no known methods or data for determining best values of the parameters in the Lennard-Jones potential. We have chosen 2 kcal/mole (0.087 eV) as a representative value for the Ar-Ag atomic bond, 0.027 eV for Ne-Ag, and 0.0074 for He-Ag, estimates whose accuracy we have no way of assessing. The variation with gas species is probably exaggerated in our estimates since we have made the atom-atom bonding energies (ϵ) proportional to the corresponding values for homogeneous (e.g., Ar-Ar) interactions,[13] instead of employing the usual geometric-mean combining rule. We

We have used 3.10, 2.80, and 2.68Å for the corresponding Lennard-Jones internuclear diameters, σ, in each of the noble gas interactions with Ag atoms. It is indeed unfortunate that we know of no better data for these potentials, since they may be producing significant errors in predicted results. Two cases for neon at 300°K have been run with greatly reduced interatomic binding energies to assess the possibility that the assumed values may be in error. It may be possible in the future to infer better interatomic potentials by comparing the present calculations with experiments. The accepted bulk value of 4.08Å was used for the lattice spacing (i.e., the edge of a unit cube).

Many different input conditions have been studied for the noble gases He, Ne, and Ar incident on single-crystal Ag surfaces that were maintained at 560°K. Most of these have involved Ne, which best fits the assumptions of the theory and the behavior of the computation at thermal energies. Since in low energy cases trapping was quite likely, a very large number of incident trajectories was sometimes necessary to get a statistically meaningful number of reflected trajectories. Two cases of Ne on Ag (100) were studied at 5600°K to examine the importance of surface structure relative to the (111) surface used in the balance of the cases.

RESULTS

The probability of trapping for many of the cases is shown in Fig. 3. Although this behavior is typical of that described in previous theoretical treatments of gas-surface interactions,[4,5,9] it is in direct conflict with the inferences drawn by the various experimenters, in particular Saltsburg and Smith.[1]

With this exception, the mean values of interaction parameters shown in Figs. 3 through 7 do not reflect anomalous behavior. The most notable feature is the qualitative agreement between trapping probability and energy exchange as predicted[4] and as found in the present numerical experiments. None of the present data was used in formulating the prediction equations. The predictions indicate quite a sharp change from positive to negative energy exchange at $T_i = T_w$, a change that is reflected well in the results (Fig. 4). The data for various incident angles (Fig. 7) indicate that the predicted minimum for energy transmitted to the lattice (E_ℓ/E_i) at an incident angle of about 130 degrees is also suggested by the data. The increase at angles of more glancing incidence is due to the increasing effect of the attractive potential, while that at more normal angles is due to the more direct collisions.

The most important feature in the spatial distribution results is a tendency to divide into separate modes of scattering for high and low incident energy. The low-energy mode shows trends that are consistent with experimental observations and the predictions

of the Logan-Stickney-Keck hard cube theory. The lobes become broader and usually move closer to the surface normal as E_i decreases (see Fig. 8, and compare with Fig. 6 of Ref. 1). This we call "thermal scattering" because it is generated primarily by thermal oscillations in the target lattice, which are relatively more important at low E_i/kT. The high-energy mode gives an opposite trend, namely that the direction of maximum intensity moves away from the surface (toward the normal), and the lobe becomes more broadly scattered as E_i increases. We call this behavior "structure scattering," because it is, we believe, a result of the increased apparent roughness of the atomic configuration of the surface as the penetration of the surface potential field becomes greater with increased energy. The net result of these competing mechanisms is not easily described, especially in view of the statistical fluctuations that are known to be present[5]. Figures 8 and 9 show the flux patterns in the plane of incidence for two different Debye temperatures at 130° incident angle and several energy levels. Since the magnitudes of the flux maxima decrease as the reflected lobes become more broadly scattered both in and out of the incident plane, we get from these results a rough overall view of the interactions. Figures 10 and 11 show the corresponding information plotted as a function of incidence angle for two incident energies. Figure 2 shows that alternative samples could have made these trends appear even more strongly.

In most of the cases for moderately high E_i we find in a single scattering pattern at least vestiges of two separate flux maxima in the plane of incidence, one of these usually lying above, the other below the specular ray. These maxima may be called "rough" and "smooth" scatterings, since they appear to correspond to different classes of collision with the surface atoms. The "rough" peak represents a greater deflection from the original direction of motion and is usually accompanied by a greater degree of energy exchange. We should expect this behavior to be typical of small impact parameters or multiple collisions. The "smooth" peak represents a more glancing interaction, typical of larger impact parameters, and it usually results in a smaller energy exchange. Sometimes one peak completely dominates the other; sometimes additional maxima are observed. But the tendency of the maxima to fall into two distinct classes within a single case is quite strong. No satisfactory explanation for this behavior has yet been discovered, although there appears to be some connection between the rough peak and the structure scattering as well as between the smooth peak and thermal scattering. No evidence of this behavior is present in the experimental data available to date, nor is this behavior strongly indicated in the present results in instances in which E_i is either extremely high or within the range of of the experiments.

It was postulated that these peaks were the product of some particular lattice configuration or orientation. A case was studied

which could also be handled by the Jackson approach,[9] namely interaction with the Ag (100) surface. This involved two cases, one with a typical set of random azimuth angles (φ_i), the other with the incident planes parallel to the direction of closest packing on the (100) face. It is evident from Fig. 12 that multiple peaks are to be expected for a broad range of geometries.

The scattering of He and Ar present some interesting contrasts with the Ne cases. The high velocity, low binding energy, and small size of the He atom make it act like a very high energy Ne atom, while the opposite effects make Ar act like a lower energy Ne atom. The hard-sphere mass ratio effect clouds this simple picture considerably, but it is still a useful rule. Out-of-plane scattering of He is greater than that of high energy Ne, because the former resolves the lattice structure better; conversely, high energy Ar is more closely confined to the incident plane than is low-energy Ne. An important caveat must be attached to the He data, viz., that they are in the range where quantum effects may predominate. If they do, the validity of these data is dubious at best. Figure 13 shows two in-plane flux patterns for He and for the only Ar case in which the untrapped fraction was large enough to give a scattering pattern. We could not reproduce any data for Xe , because trapping would have been complete.

The amount of information that can be extracted from each case is so great that it is impossible to present all of it. Addi-

tional features that are most instructive are the relative broadness of the lateral scattering and the relative energy at various exit angles. As a gross generalization, it may be stated for $\theta_i < 140°$ that most lobes are locally nearly symmetric about an axis through their maximum, even for multilobe patterns. There is a tendency toward greater out-of-plane scattering as θ_i increases, giving a roughly constant lateral momentum pattern (see Figs. 6 and 7). Both in- and out-of-plane broadness is therefore crudely indicated by the relative amplitude of each maximum. Figure 14 shows one of the cases for which this rule was least applicable. The indicated velocity spectrum is far more complex, showing new types of variations almost every time a new case is introduced, but the relative magnitudes of velocity within a scattering pattern do not change as drastically as do the flux magnitudes. The clearest trends in exit velocity occur at the high and low extremes of incident energy. One high and two intermediate energy cases are shown in Fig. 15. At high E_i, the energy transfer correlates fairly well with the angle through which the incident ray has been turned, which tends to give a maximum energy transfer for a maximum deflection (back toward the incident) and a minimum transfer at minimum deflection (along the surface). The out-of-plane scattering follows nearly the same curve. This behavior strongly supports a hard-sphere limit behavior such as would be expected[5] at high E_i ($E_\ell/E_i \approx \cos^2\psi$, where ψ is the angle through which the velocity is deflected). At low E_i/kT_w, we find that the greatest

energy transfer (now from the lattice to the gas atom) occurs for those atoms exiting near the surface normal, while in some cases those exiting nearer the surface tangent actually lose energy. In this range there is a systematic change in energy transfer with each increase in φ. The 700 and 2800° cases of Fig. 15 are hybrids of both types, typical of intermediate energies.

We have been able to produce successful computations for only three cases presented by Saltsburg and Smith: He at 300 and 1400°K and Ne at 300°K; all at 130° incidence (i.e., 50 degrees from the normal). They have found He specular "at all incident angles and temperatures," and show a very sharp specular trace at 300°K. We find a two-lobe pattern (one of them specular, the other more normal) which is quite broad at both 300 and 1400°K. One might explain this disagreement by recalling that de Broglie wavelengths for He (300°K) are about 0.8Å, or definitely significant compared to collision lengths on the lattice, which according to our previous determinations[4] might be as low as .3Å. Helium at 1400°K and neon at 300°K (both have $\lambda \sim .35$Å) are less easily explained away. Saltsburg and Smith show a Ne trace that has a half-amplitude width of about 35 degrees in the incident plane; our value is about 76 degrees (see Fig. 16). Their peak is about 5 degrees below the specular (i.e., toward the normal); ours about 20 degrees below. Although this disagreement raises many questions, it certainly is not alarming in view of the enormous

violation of the range of validity that was necessary for the calculations needed to produce the results. Before a final judgment is made on either theory or experiment, a much greater overlap of applicable conditions must be available.

Despite the paucity of corresponding cases, it may be useful to postulate causes for the observed disagreement that would yet be consistent with the features that do agree between theory and experiment. The most probable of these causes is a gross overestimate of the gas-solid interatomic binding energies. This overestimate would also explain the discrepancy in trapping probabilities between experiment and calculation. We have explored this possibility in two additional runs for neon in which the Lennard-Jones binding energies are arbitrarily reduced by factors of 5 and 10 from their originally assumed values of 0.027 eV. The results shown in Fig. 16 indicate that a large reduction in ϵ might make the calculations more realistic, but this comparison involves too much adjustment to be conclusive.

CONCLUSIONS

Although the computational requirements of our numerical calculations have demanded that we use smaller samples than desirable, we think that it is possible with the present interpolation technique to draw conclusions as to the gross characteristics of spatial distributions of reflected molecules. We anticipate that

future experiments will provide guidelines for improving this type of calculation, in particular by providing better indications of interatomic binding energies and actual surface configurations.

The conflicts between present results and published experimental data are in our high trapping probability for heavy gases at lower incident energy, and the width of the scattering patterns for the few questionable cases that can be compared directly. It cannot now be established whether we have an incorrect feature in our model, are using binding energies that are much too large, or have drawn misleading inferences from the experiments. At present, the second of these appears most likely. We do find several trends confirmed in the experiments. At low E_i the thermal scattering mechanism is the dominant one, giving broader and more normal exit distributions as T_w/T_i increases. At $T_i < T_w$ the particles emitted in the more normal directions tend to acquire greater energies than those nearer the surface. Out-of-plane scattering generally tends to reflect the character of the in-plane scattering. Scattering maxima can occur either above or below the specular ray, usually lying closer to the surface (i.e., supraspecular) for E_i's that are large compared to wall thermal energy, but not so large as to allow the atoms to penetrate deeply into the repulsive portion of the lattice atom potential field.

We also find several trends that are outside the accessible range of existing experiments. Scattering by the lattice structure,

in which the distributions become more broadly dispersed and move slightly more toward the normal, becomes important as E_i increases to values very large compared with $\epsilon \cos \theta_i$. For instance, at about 8 eV incident energy and 130° incidence, a Ne atom should penetrate the Ag potential field to about the point where the effective atomic diameter is equal to the apparent grid spacing ($\sqrt{2}\, d \cos \theta_i$, where $2\,d$ is the unit cube edge) of the fcc (111) lattice. The atomic configuration should then appear quite rough. This condition corresponds roughly to the highest energy tried herein (44,800°K). We feel structure scattering is significant for He at all energies tested, for Ne above about 5000°K, and for Ar and larger atoms only at very large energies. Note that the few cases run with He and Ar confirm this expectation, with He lying more below the specular (i.e., toward the normal), while Ar lies more above the specular relative to Ne at similar energies (cf. Fig. 13). This trend is opposite to what would be shown if thermal scattering were dominant,[8] but is the same as that of Goodman[5] for very high E_i.

Another feature that is outside current experimental experience is the frequent occurrence of multiple peaks in the flux patterns. Some of these may be products of the statistical method but most fall into a consistent pattern that strongly indicates a legitimate phenomenon. This phenomenon appears related to structure scattering since it occurs again at very low E_i with He

and is totally absent in our sparse data for Ar, even at very high E_i. Multiple peaks occur on the (100) surface as well as on the (111), and can be produced with a constant azimuth angle in the input (see Fig. 12). The analytical model that should best show this behavior is Erofeev's,[6] but our numerical evaluations of his theory do not reflect this behavior. If multiple scattering is a genuine physical rather than a merely statistical effect, it requires a more complex geometry than that incorporated in the Erofeev theory to display it.

Finally, it is encouraging to theoreticians to note that the cases tested at high E_i show a scattering strongly suggestive of hard-sphere mechanics. The energy change correlates well with the angle through which the gas particle has been deflected, regardless of how far out-of-plane the final path. This indicates collision times that are very brief compared to oscillator natural periods and further substantiates the hard-sphere limit behavior inferred a priori by many authors, and by the author's analysis[4] of average energy exchange. Goodman's calculations[5] show this behavior clearly.

ACKNOWLEDGMENTS

I should like to thank the many people who helped with this work, in particular Alex Bogan, Calvin Weiser, and Chou Li, who were my coauthors of previous papers on this subject, and helped in the early development of the method. I should also like to thank Benjamin Kirkup, Jr., for his help in carrying out the calculations.

REFERENCES

1. H. Saltsburg and J. N. Smith, Jr., J. Chem Phys. 45, 2175 (1966): Their techniques are also employed in several other papers, such as J. N. Smith, Jr., and H. Saltsburg, J. Chem. Phys. 40, 3583 (1964); H. Saltsburg, J. N. Smith, Jr., and R. L. Palmer, in Rarefied Gas Dynamics, Supplement 4, Vol. 1, C. L. Brundin ed., 223, Academic Press, New York (1967), hereinafter denoted by RGD (1967)
2. J. J. Hinchen and E. F. Shepherd, in RGD (1967) p. 239.
3. A large percentage of the modern efforts to achieve reliable measurements of gas-surface interactions by molecular beam methods are reported in RGD (1967) Vols. 1 and 2. Some additional reports are forthcoming in Proc. Symp. on Fund. of Gas-Surface Interactions, San Diego, Cal., December 1966, H. Saltsburg, ed. (to be published).
4. R. A. Oman, A. Bogan, Jr., C. H. Weiser, and C. H. Li, AIAA J., 2, 1722 (1964); _____, _____, and C. H. Li, in RGD Supplement 3, Vol. 2, J. H. de Leeuw, ed., 396 (1966); R. A. Oman, in RGD (1967) Vol. 1, p. 83; _____, AIAA J. 5, 1280 (1967). The first of these describes the basic calculation method, the second some early monatomic results, the third an extension to diatomic gases, and the last presents studies of several secondary phenomena (surface contamination, lattice structure, thermal motion) along with a simple phenomenological model which correlates

energy exchange and trapping probability for large ranges of the various interaction parameters with the results of the full computer calculations. This is the same model which is used to generate predictions for the present cases.

5. F. O. Goodman, RGD (1967), Vol. 1, p. 35; Surf. Sci. 7, 391 (1967).
6. A. I. Erofeev, Inzh. Zh. 4, 862 (1965). English Trans. in Grumman Research Department TR-38, J. Brook (1966); _____, Zh. Prikl. Mekhan. i. Tekhn. Fiz. No. 3 (1966). English Trans. in Grumman TR-39, J. Brook (1967).
7. L. M. Raff, J. Lorenzen, and B. C. McCoy; J. Chem. Phys., 46, 4265 (1967).
8. R. M. Logan, J. C. Keck, and R. E. Stickney, RGD (1967), Vol. 1; see also R.E. Stickney, J. Chem. Phys. 44, 195 (1966).
9. D. Jackson, Ph.D. Thesis in preparation, University of Toronto, Ontario. We are grateful to Mr. Jackson for transmitting to us some of the qualitative results of his research thus far.
10. R. J. Madix and R. A Korus, Private Communication (1967).
11. F. O. Goodman, RGD (1966) Vol. II, p. 366; Surf. Sci., 5, 283 (1966).
12. H. B. Lyon and G. A. Somorjai, J. Chem. Phys., 44, 3707 (1966).
13. Potential parameters from many sources are tabulated by J. O. Hirschfelder, C. F. Curtiss, and R. B. Bird in Molecular Theory of Gases and Liquids, p. 1110, Wiley, New York, 1954.

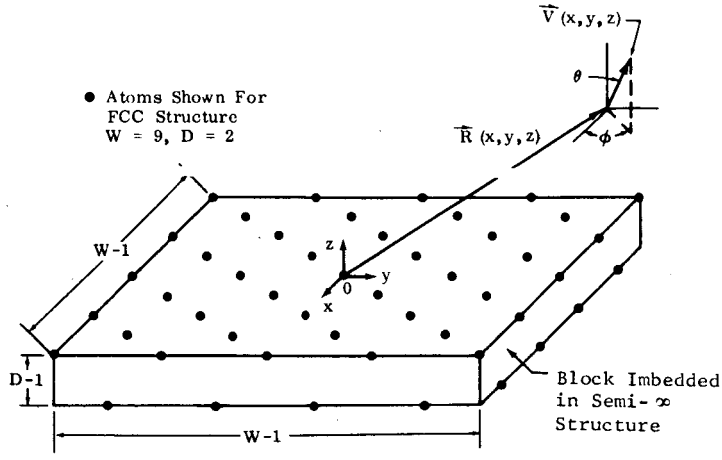

Fig. 1 Coordinate System and Lattice Atom Configuration for Trajectory Calculations. Output angle φ is referred to plane of incidence.

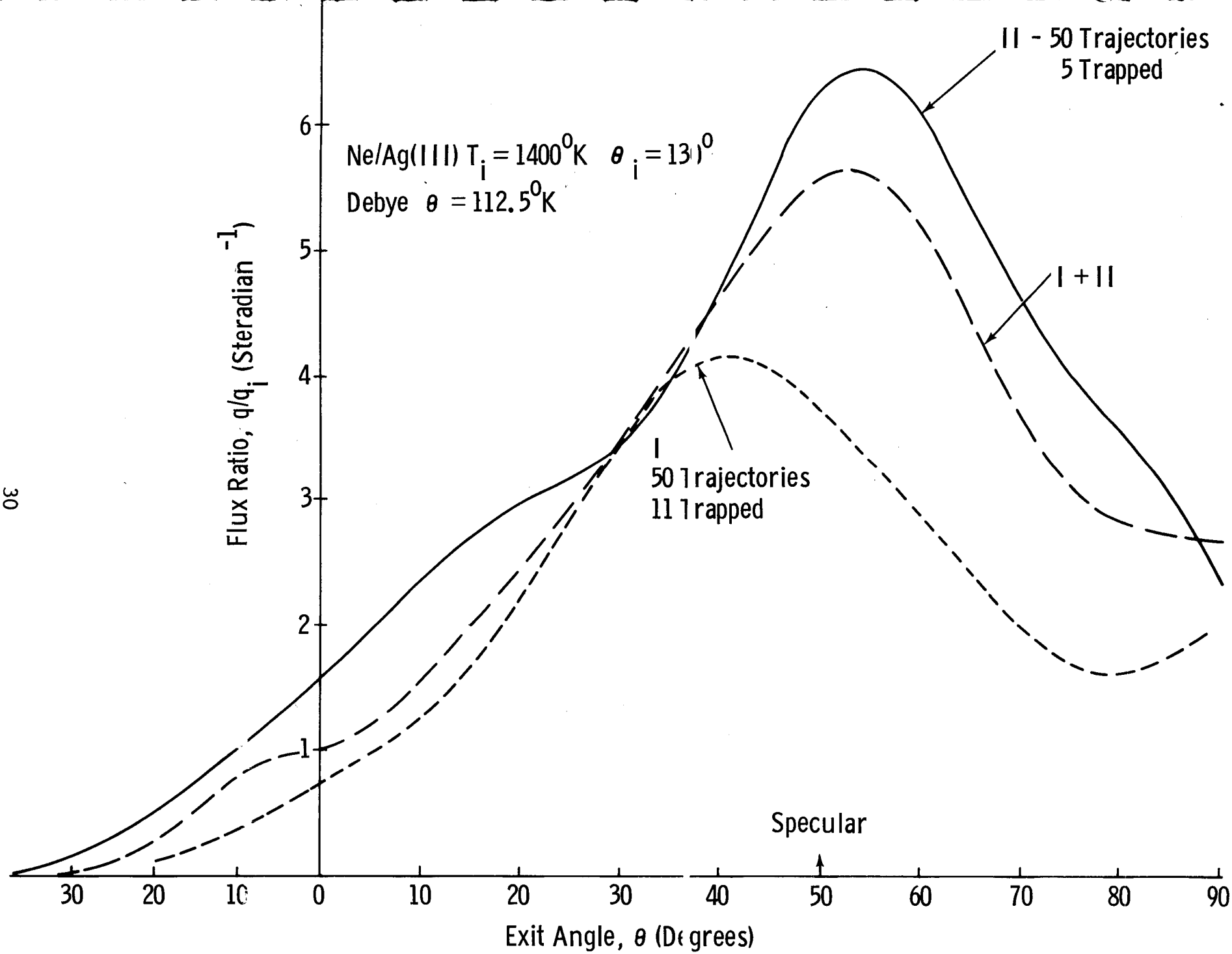

Figure 2a Comparison of Indeper dent Statistical Samples

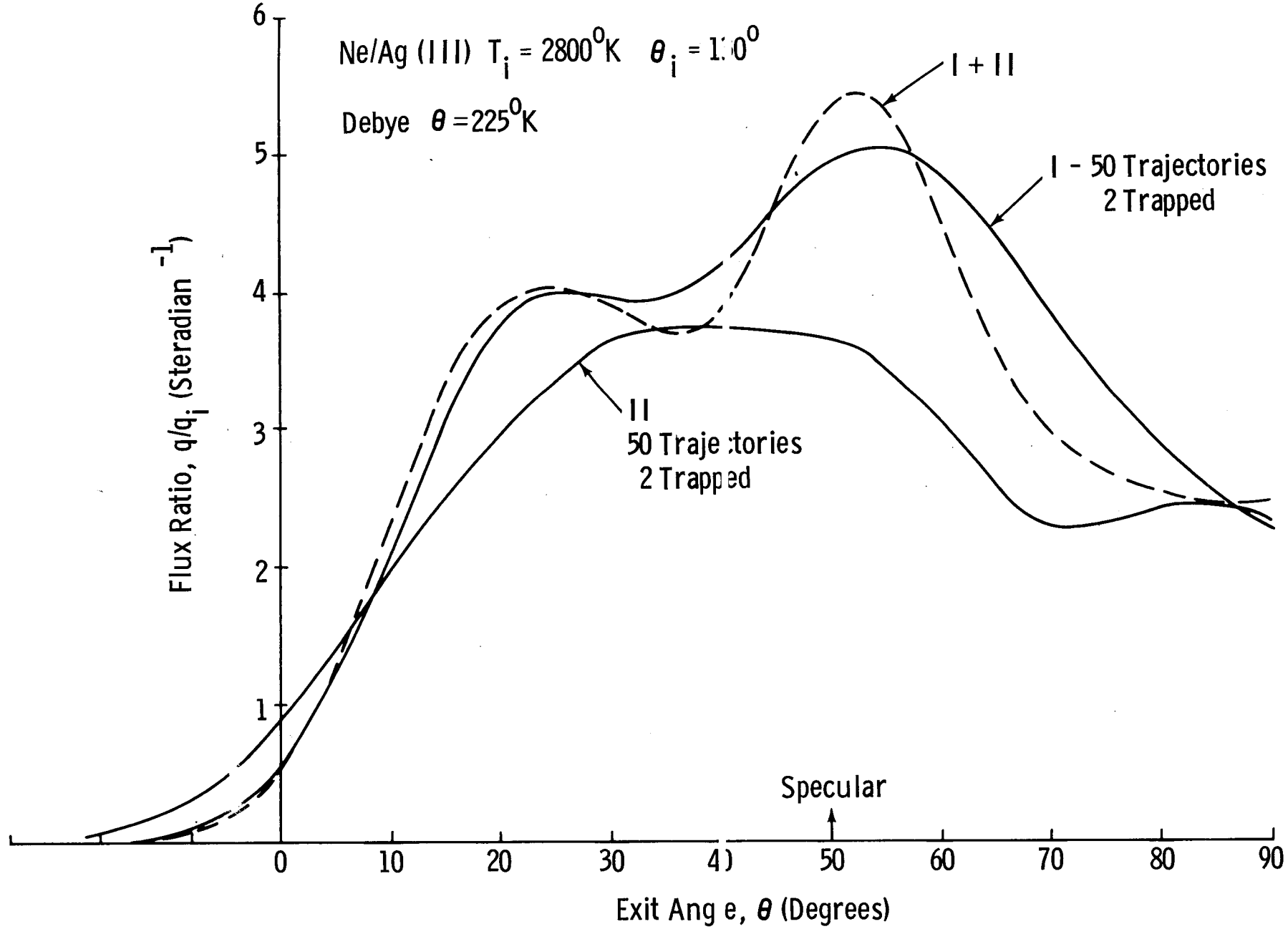

Figure 2b Comparison of Indepe ndent Statistical Samples

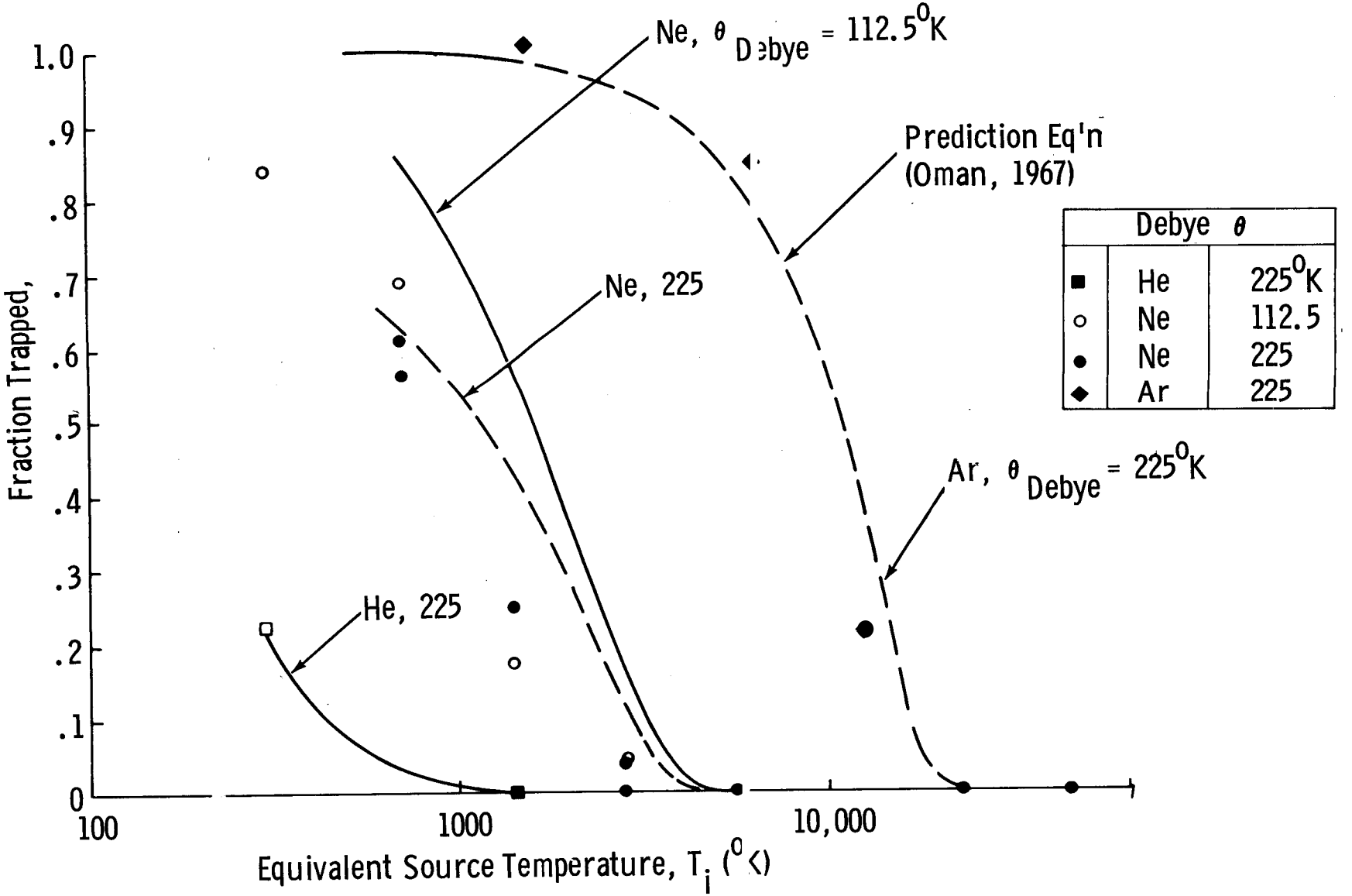

Figure 3 Trapping on Silver (111) at 130° Incidence

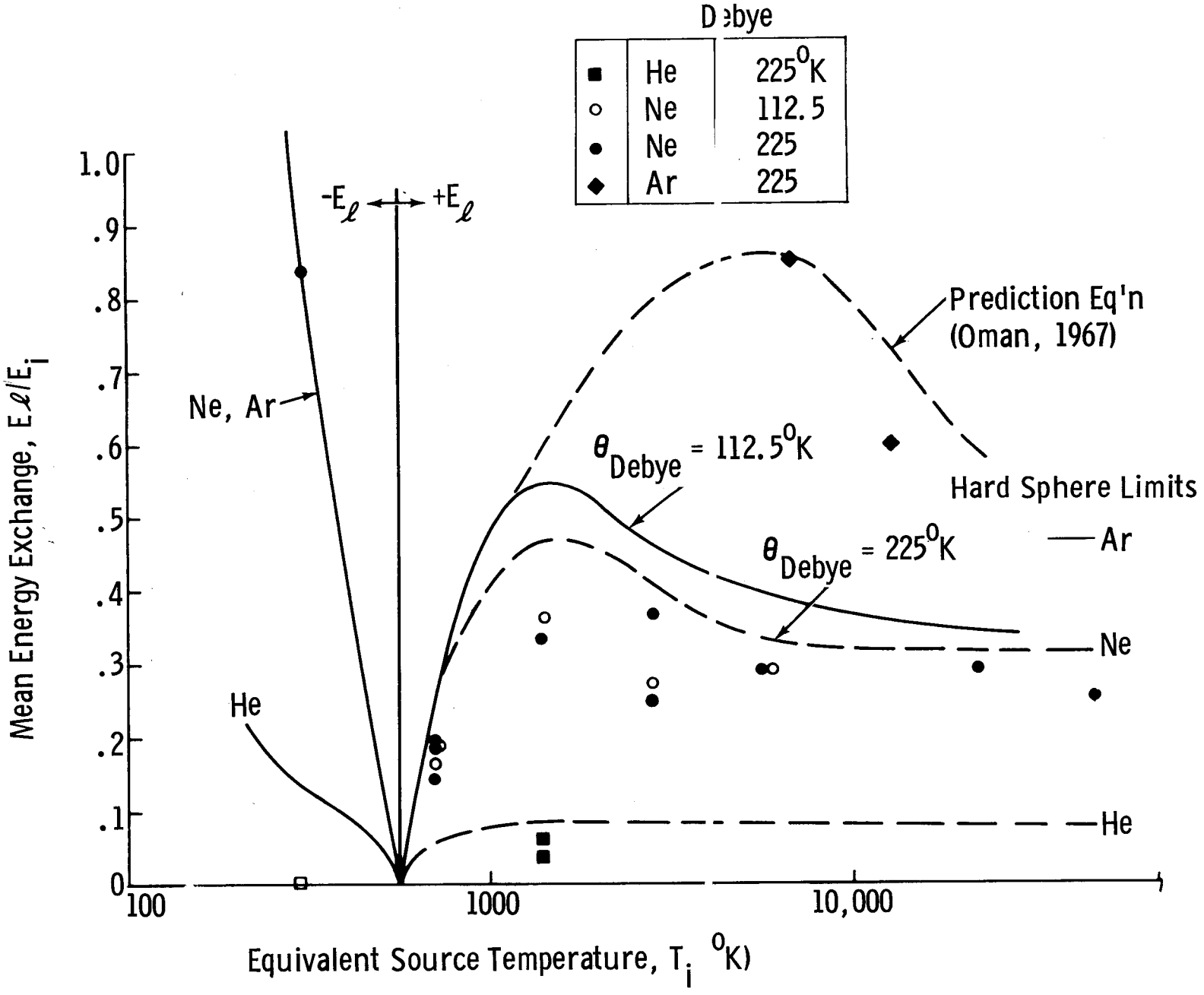

Figure 4 Energy Exchanged with Silver (111) Lattice at 130° Incidence

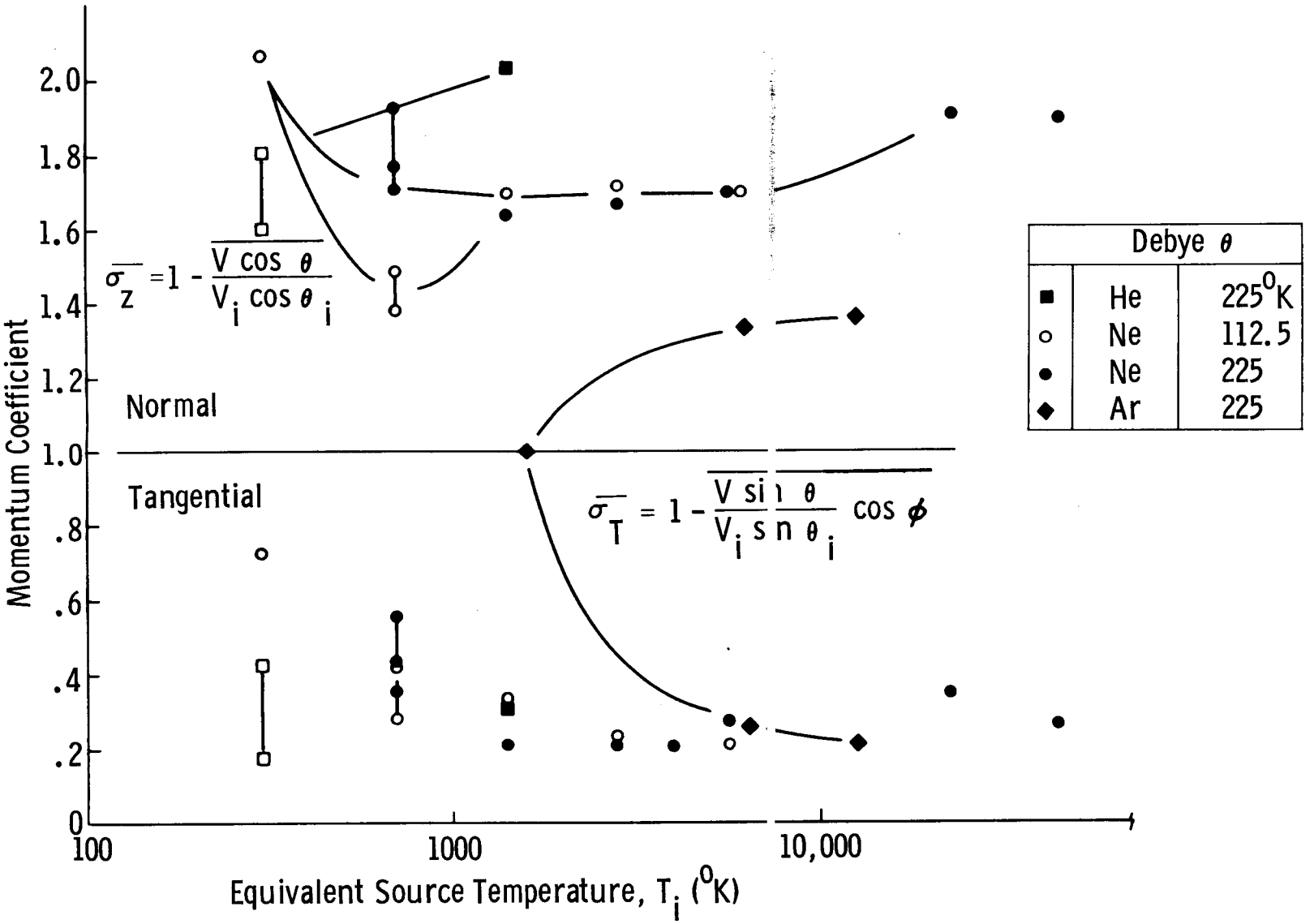

Figure 5 Mean Momentum Coefficie nts at 130° Incidence

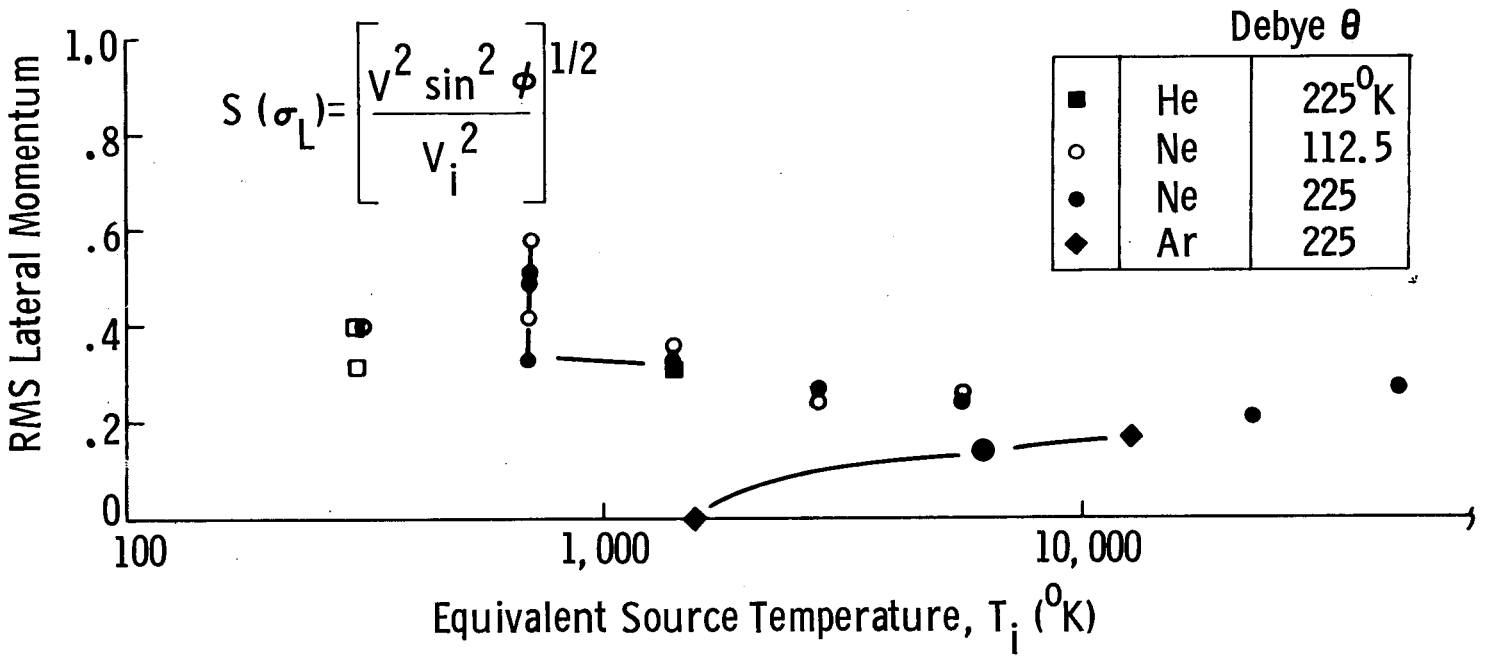

Figure 6 RMS Lateral Momentum Coefficient at 130° Incidence

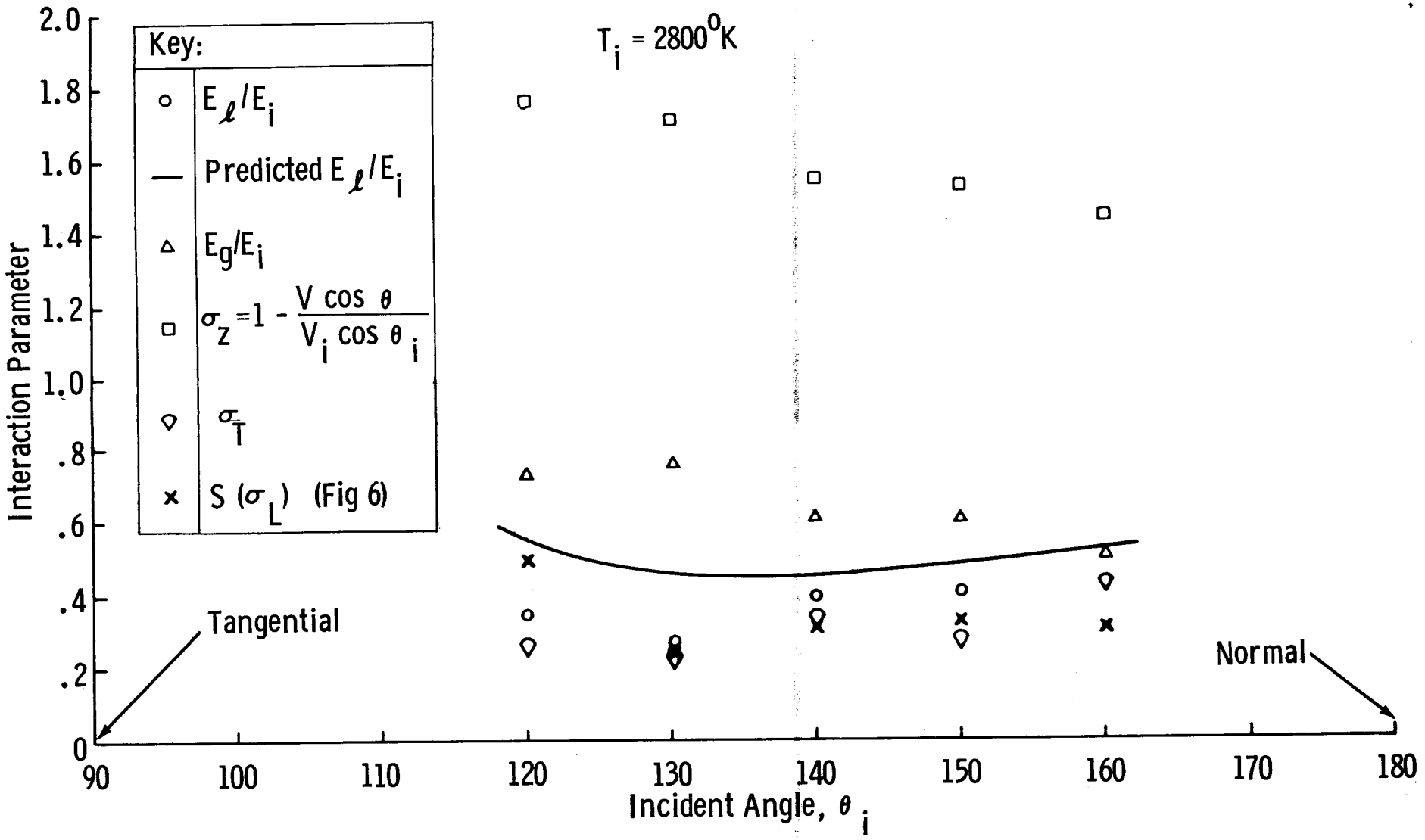

Figure 7 Mean Interaction Parameters for Neon on (111) Silver at Different Incident Angles

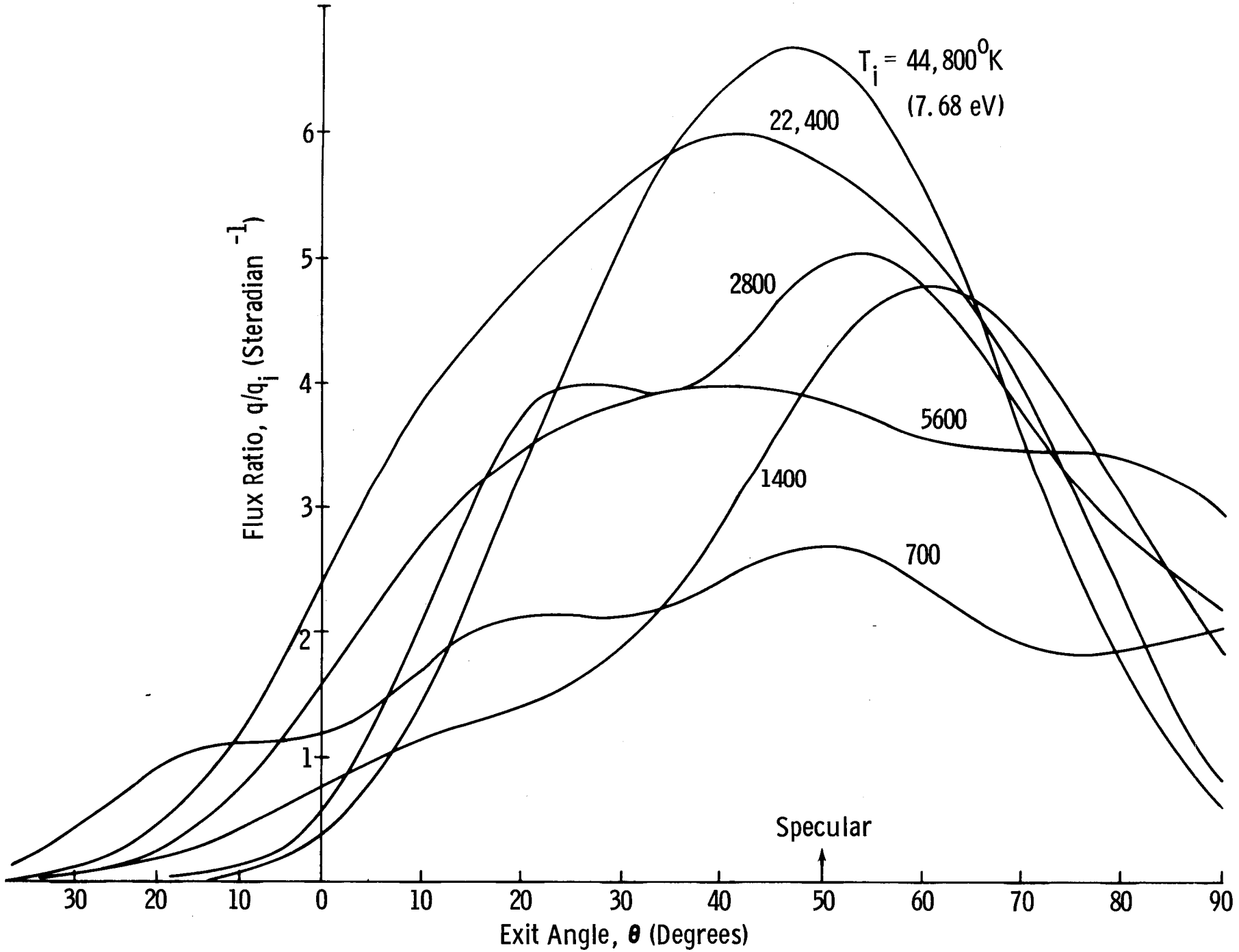

Figure 8 Incident - Plane Flux for Neon at 130° Incidence
Ag (111) Debye θ = 225°K

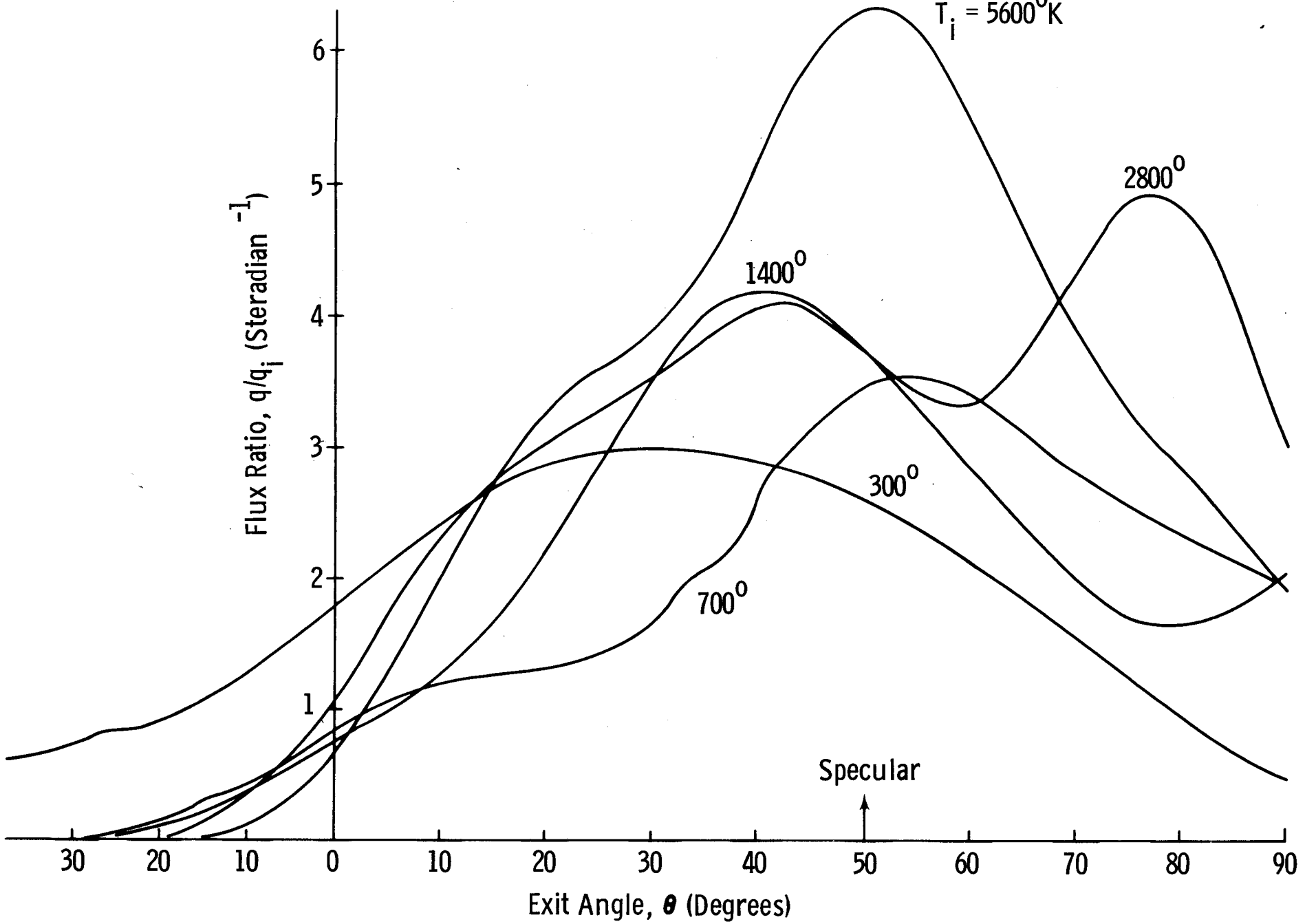

Figure 9 Incident - Plane Flux for Neon at 130^0 Incidence
Ag (111) Debye $\theta = 112.5^0K$

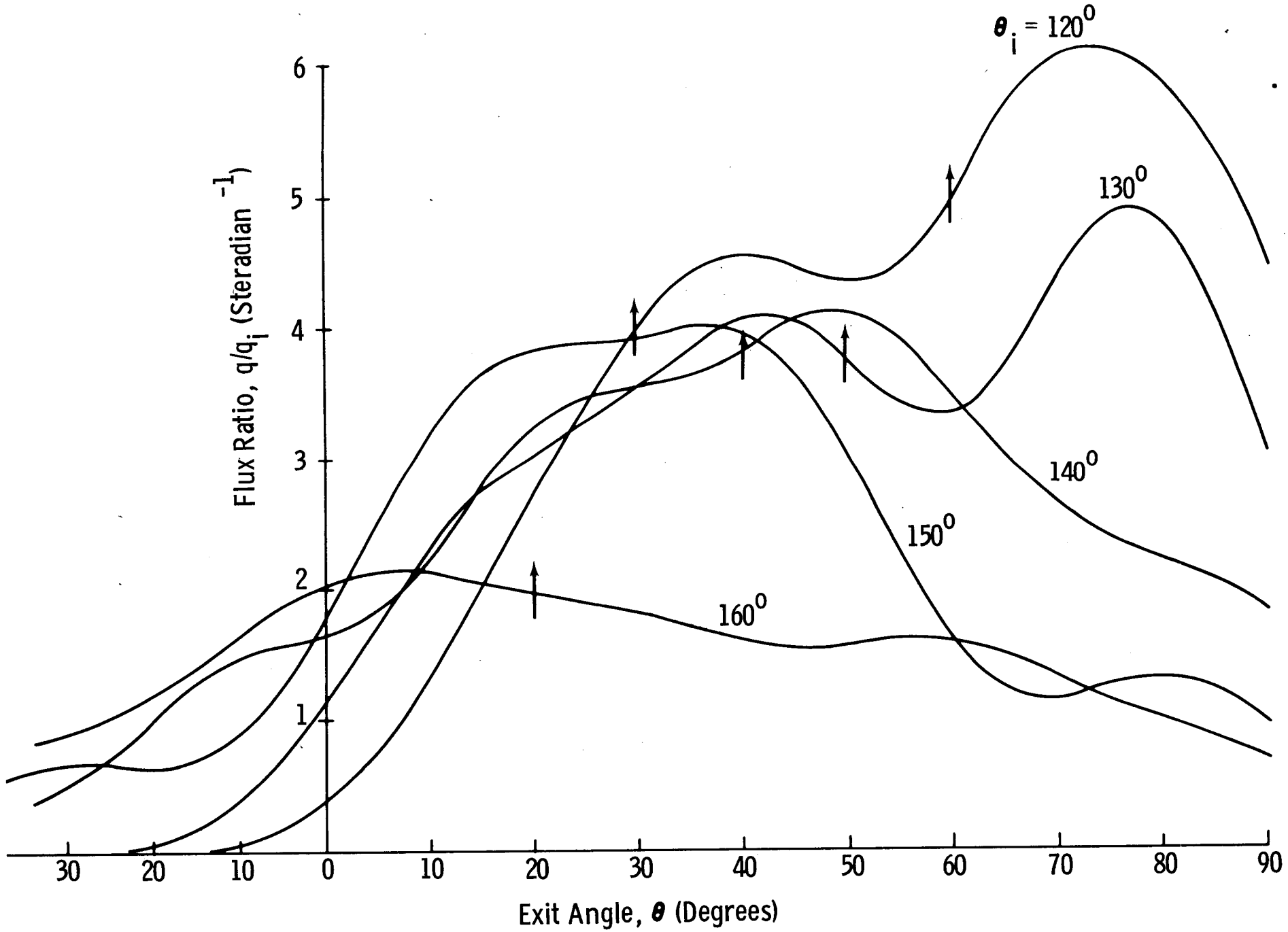

Figure 10 Incident - Plane Flux for Neon at 0.48 eV
Ag (111) Debye θ=112.5^{0}K

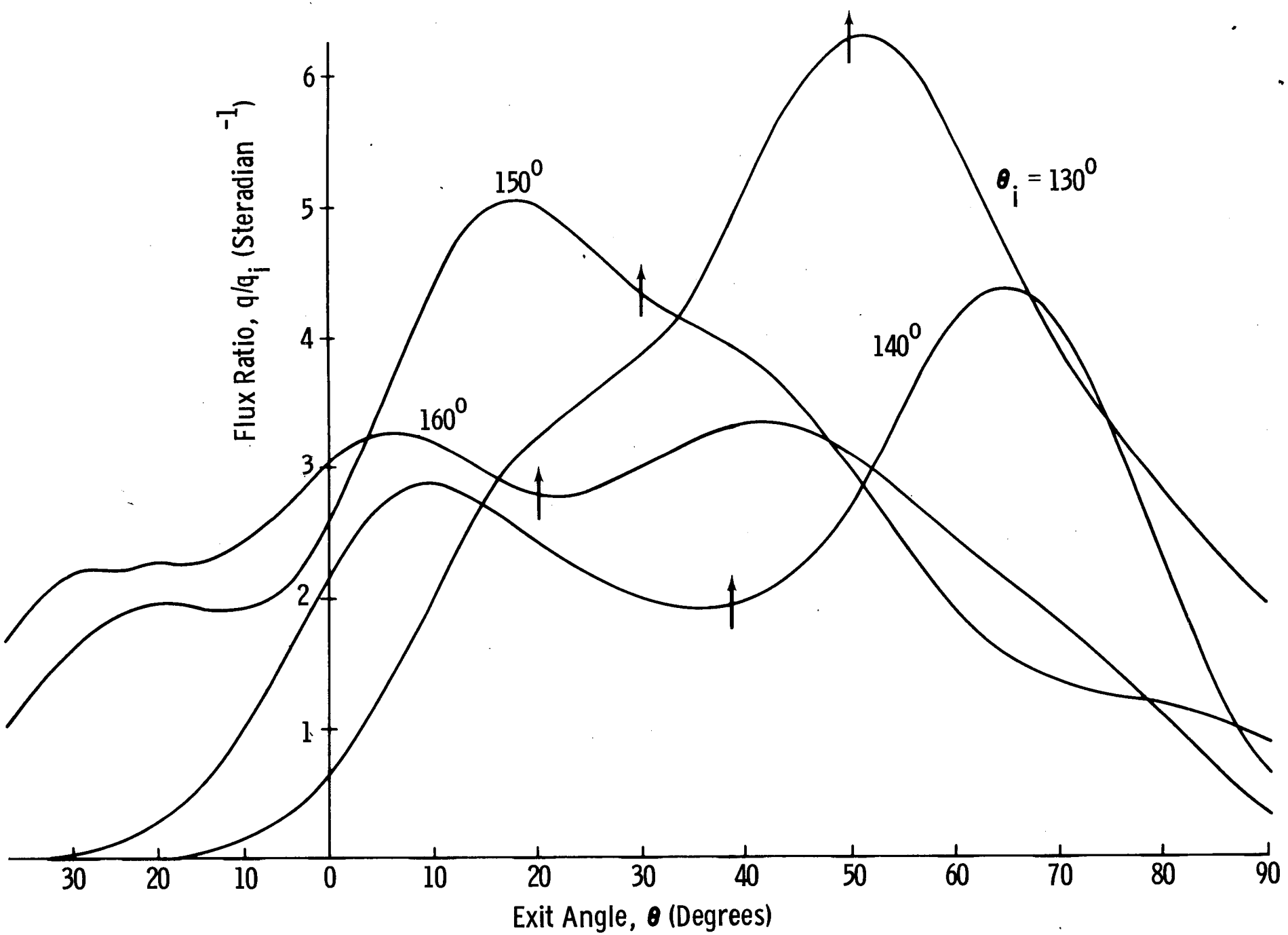

Figure 11 Incident - Plane Flux for Neon at 0.96 eV Ag (111)
Debye θ = 112.5°K

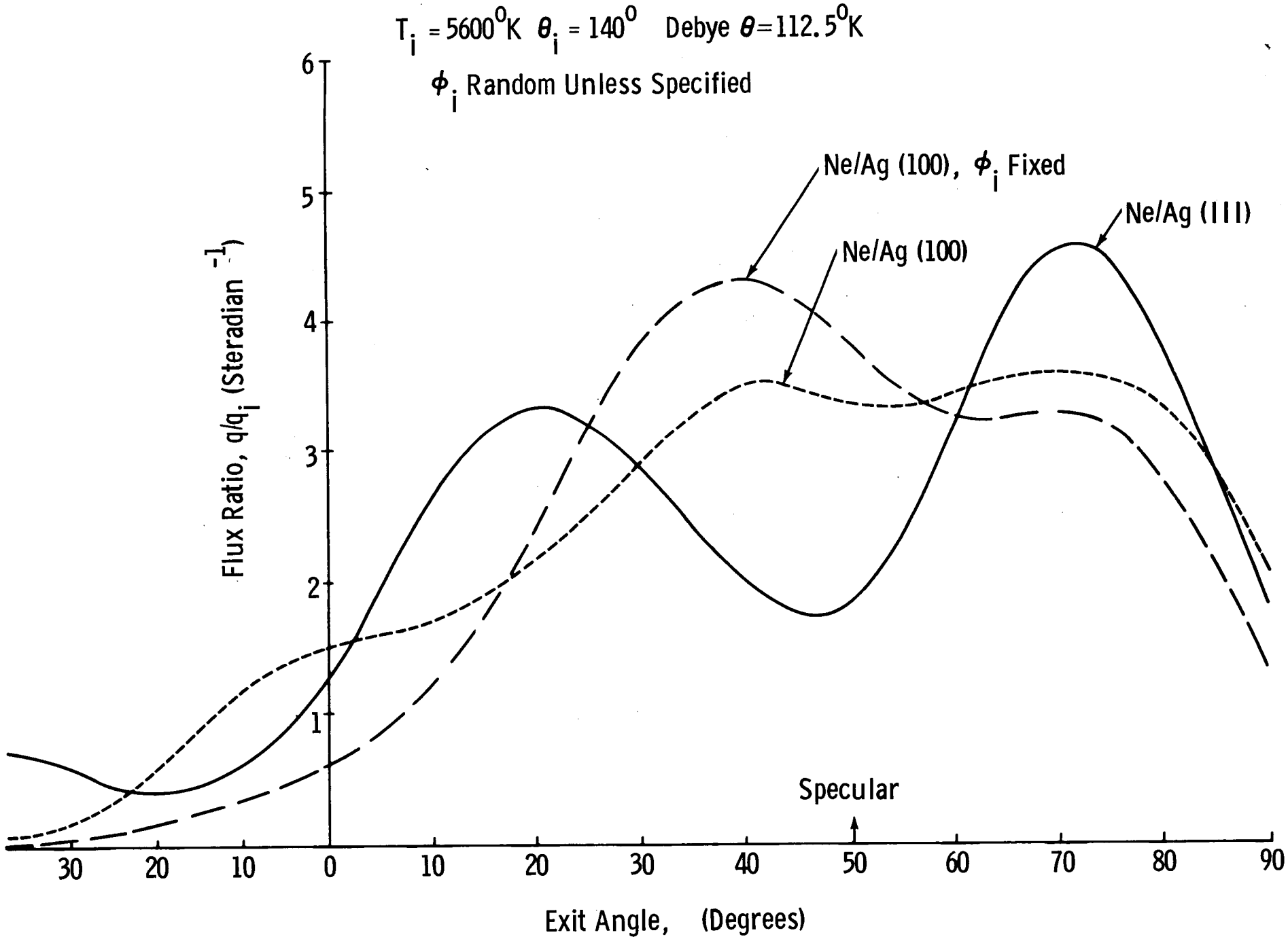

Figure 12 Effect of Structure and Random Azimuth

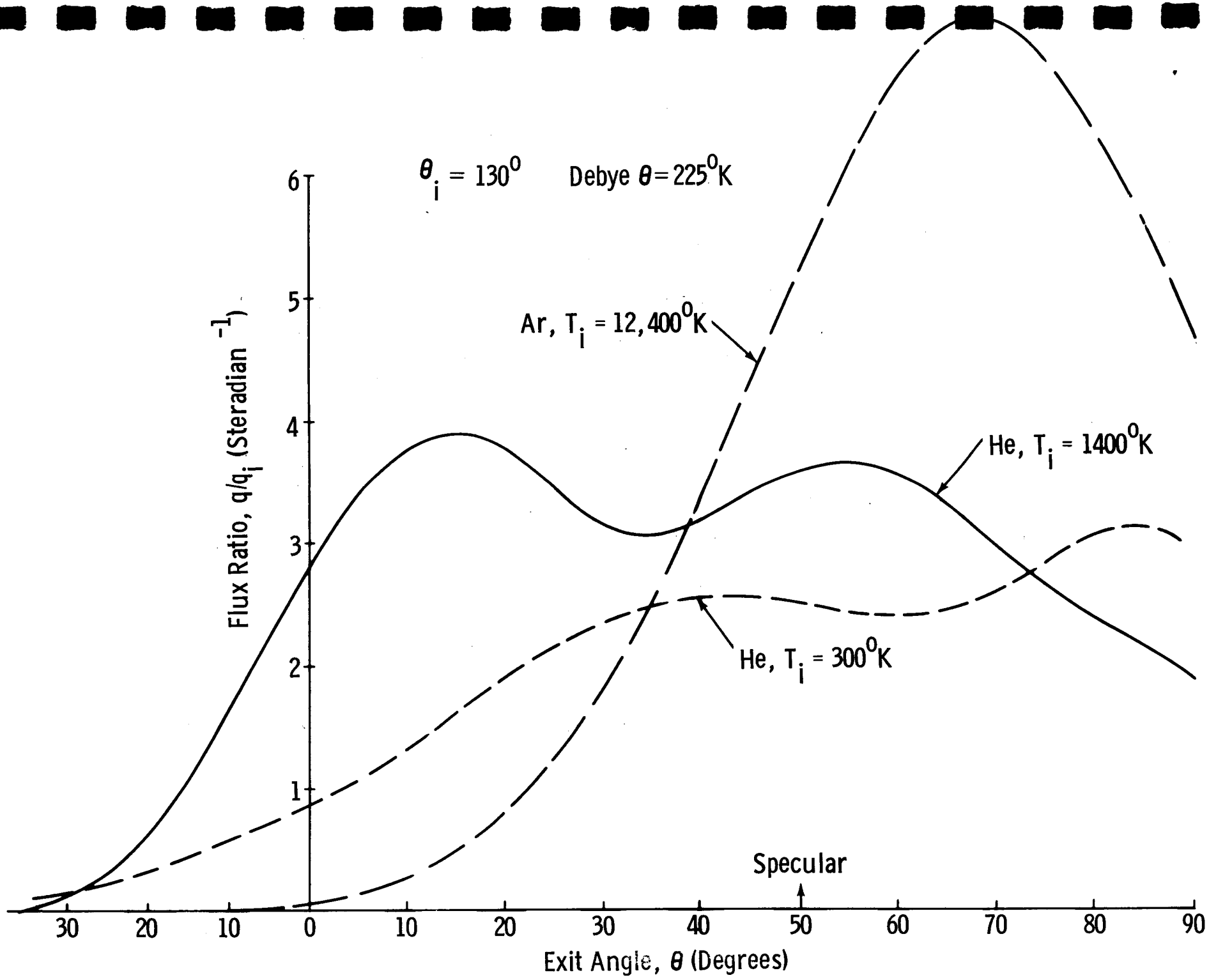

Figure 13 Comparison of Scattering for Different Gases on Silver (111)

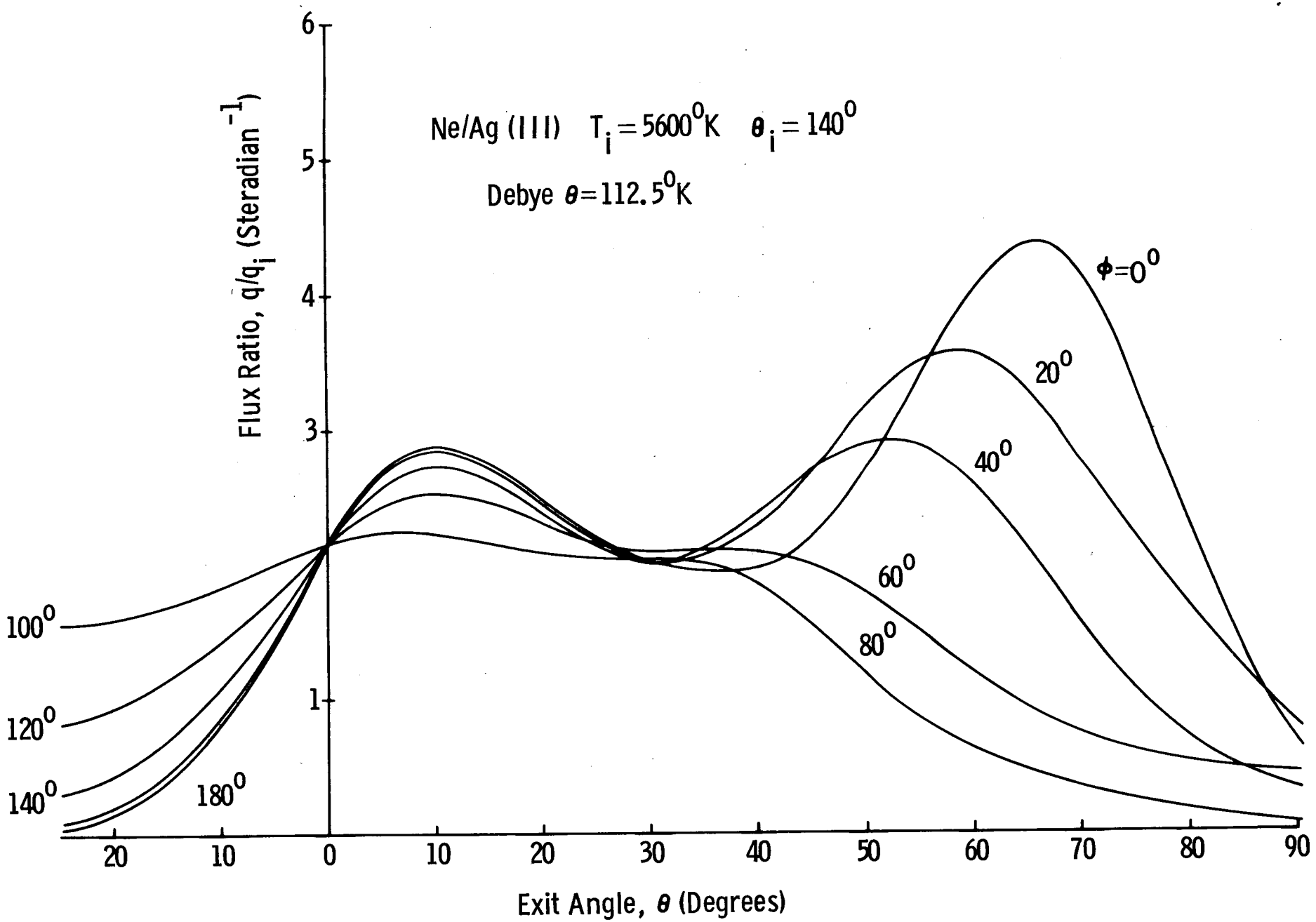

Figure 14 Azimuthal Variation of Flux Ne/Ag (111)

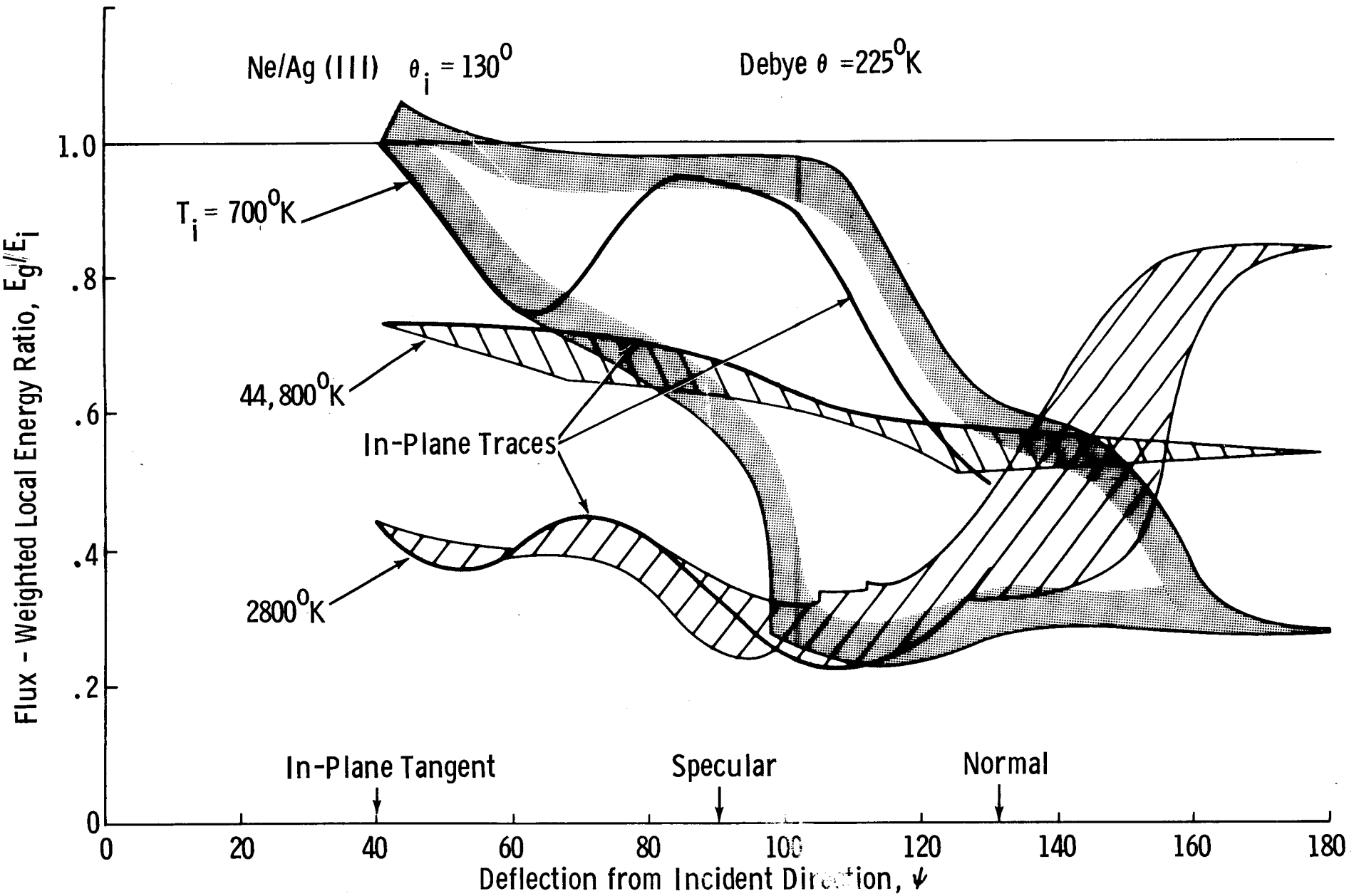

Figure 15 Envelopes of Local Energy vs Deflection Angle

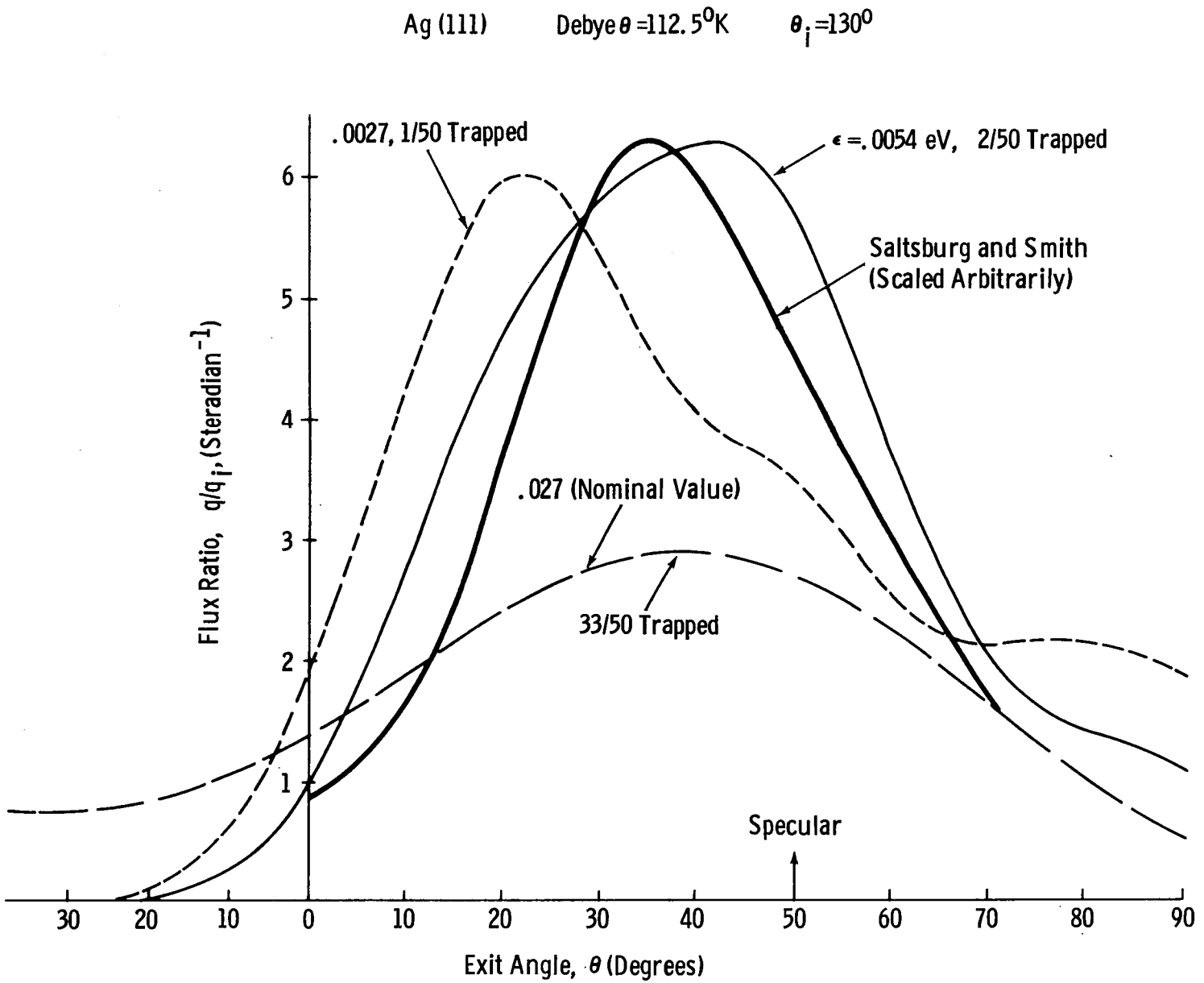

Fig. 16 Comparison of Neon Scattering At 300°k With Various Assumed Binding Energies